JOURNAL OF MATERIALS SCIENCE 29 (1994) 5321–5326

Microstructural development and mechanical properties of pressureless-sintered SiC with plate-like grains using Al_2O_3–Y_2O_3 additives

SEUNG KUN LEE, YOON CHANG KIM, CHONG HEE KIM
Department of Ceramic Science and Engineering, Korea Advanced Institute of Science and Technology, 373-1 Kusong-dong, Yusong-Gu, Taejon 305-701, Republic of Korea

Dense SiC ceramics with plate-like grains were obtained by pressureless sintering using β-SiC powder with the addition of 6 wt% Al_2O_3 and 4 wt% Y_2O_3. The relationships between sintering conditions, microstructural development, and mechanical properties for the obtained ceramics were established. During sintering of the β-SiC powder compact, the equiaxed grain structure gradually changed into the plate-like grain structure that is closely entangled and linked together through the grain growth associated with the $\beta \rightarrow \alpha$ phase transformation. With increasing holding time, the fraction of $\beta \rightarrow \alpha$ phase transformation, the grain size, and the aspect ratio of grains, increased. Fracture toughness increased from 4.5 MPa $m^{1/2}$ to 8.3 MPa $m^{1/2}$ with increasing size and aspect ratio of the grains. Crack deflection and crack bridging were considered to be the main operative mechanisms that led to improved fracture toughness.

1. Introduction

SiC ceramic is one of the promising candidate materials for high-temperature structural components in heat engines, heat exchangers, and many other devices because of its excellent oxidation resistance, strength retention to high temperature, high wear resistance, good thermal conductivity, and relatively low coefficient of thermal expansion. Prochazka's sintering of SiC in the absence of applied pressure opened up the possibility of mass production of relatively inexpensive SiC components [1].

However, SiC, as well as other ceramics, is very sensitive to defects such as pores, cracks, and large grains, which result in relatively low reliability as structural components. One of the solutions under consideration is to increase its strength by eliminating flaws or decreasing flaw sizes in the ceramics [2]. Another approach is to increase the fracture toughness by incorporating reinforcing materials and controlling the microstructure [3–7]. In many cases, incorporation of reinforcing materials has been accompanied by the degradation of desirable properties of SiC [6, 7]. Tani *et al.* [8] recently showed that the fracture toughness of monolithic Si_3N_4 can be as high as 9 MPa $m^{1/2}$ when its microstructure contains some large β-Si_3N_4 grains with high aspect ratio. (These Si_3N_4 materials are termed "self-reinforcing".) These results have caught attention in the sense that the possibility for improving the fracture toughness of the monolithic ceramics through controlling the microstructure was shown. Suzuki and Sasaki [9] developed highly toughened SiC with plate-like grains by controlling the microstructure through heat treatment using an Al_2O_3 additive. It has recently been shown that α-SiC with the addition of Al_2O_3 and Y_2O_3 could be sintered at a lower temperature (about 1850–2000 °C) than the conventional sintered, boron- and carbon-doped SiC. It has been reported that Al_2O_3 and Y_2O_3 formed a liquid phase at the sintering temperature and promoted densification by the liquid-phase sintering mechanism [10–13]. The interest in these SiC materials has grown continuously during recent years, because such materials seem to outperform the conventional SiC in both strength and toughness. However, no studies have ever tried to improve the fracture toughness through *in situ* formation of plate-like grains during sintering using β-SiC powder as a starting material in this system.

The purpose of this study was to develop the SiC ceramics with plate-like grains by pressureless sintering of β-SiC powder with the addition of Al_2O_3 and Y_2O_3. Then the relationships between sintering conditions, the $\beta \rightarrow \alpha$ phase transformation, and the microstructural development, were examined. The effects of the microstructure of liquid phase sintered SiC on the fracture strength and toughness have been discussed.

2. Experimental procedure

The starting materials used in this work were β-SiC (Betarundum, Grade UF, IBDEM, Japan), Al_2O_3 (AKP 50, Sumitomo Co., Japan), and Y_2O_3 (Grade Fine, H. C. Starck GmbH, Goslar, Germany). The SiC powder and the additives were mixed in a planetary ball mill for 12 h in acetone using Al_2O_3 balls and a

0022–2461

polypropylene container. The content of oxide additives was 10 wt % (6:4 mixture of Al_2O_3 and Y_2O_3). The additive composition was selected at near the lowest eutectic point in the phase diagram [14]. After mixing, the slurry was dried. The softly agglomerated powder was then crushed and sieved through a 60 mesh sieve. The sieved powder was die-pressed at 30 MPa and isostatically pressed at 200 MPa to densities of 58% of the theoretical limit. The resultant pressed specimens were about 3.5 mm × 4.5 mm × 30 mm in size. Sintering was performed at 2000 °C for 60, 120, 180, and 300 min in a graphite crucible that was placed in a graphite resistance furnace (Astro Industries Inc., CA, USA) in an atmosphere of flowing argon. A powder bed with the same composition as the sample was used to suppress weight loss of the sample. For comparison with the sintered SiC with addition of Al_2O_3 and Y_2O_3, the boron- and carbon-doped SiC was prepared by pressureless sintering of β-SiC powder with the addition of 1 wt % B_4C and 3 wt % C as a reference material for mechanical properties. The bulk densities of the sintered specimens were measured by the Archimede's method using deionized water as the immersion medium. The phases of the sintered SiC were analysed by X-ray diffraction with CuK_α radiation and the SiC polytypes were analysed according to the method of Ruska *et al.* [15]. The polished and etched surfaces and the fracture surfaces of the sintered specimens were observed by scanning electron microscopy. The size and aspect ratio of grains for the sintered specimens were measured using a linear-intercept method.

Fracture strength was determined by four-point bending strength using machined 2.5 mm × 3.5 mm × 20 mm bars. All specimen surfaces were polished with a 1200 diamond disc. The edges of the tensile surface were bevelled to remove edge cracks. Specimens were tested in a four-point bend fixture (inner span 6 mm and outer span 12 mm) on a mechanical testing machine at a crosshead speed of 0.5 mm min^{-1}. Fracture toughness was measured by the Vickers indentation method [16] in which specimens were polished by 1 μm diamond paste, and a 98 N load was applied.

3. Results and discussion

3.1. Microstructural development and characterization

The relative densities and the amount of phase transformation of the sintered samples are illustrated in Fig. 1 as a function of holding time. The relative density of > 98.5% was achieved with a holding time of 60 min. With increased holding time, the ratio of $\alpha/\alpha+\beta$ increased, and the major α phases of sintered bodies were the 4H polytypes. The sintering mechanism in this system was attributed to liquid-phase sintering via the formation of a eutectic melt of Al_2O_3 and Y_2O_3. Solution and reprecipitation was suspected to control the mass transport for densification [10, 13].

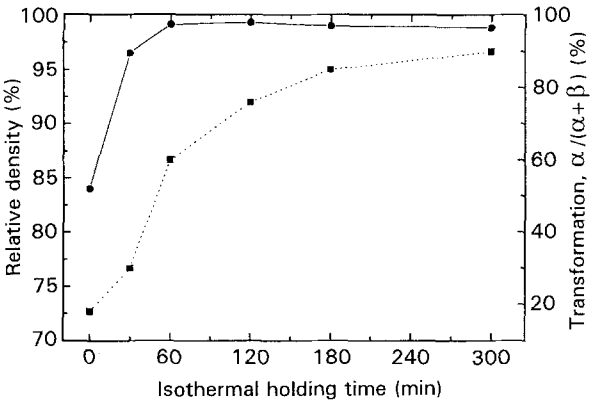

Figure 1 (●) Relative density and (■) the amount of phase transformation of SiC sintered at 2000 °C with addition of 6 wt % Al_2O_3 and 4 wt % Y_2O_3 versus holding time.

Fig. 2 shows scanning electron micrographs of the polished and etched surfaces of SiC sintered at 2000 °C for 60, 120, 180 and 300 min. With increased holding time, the microstructure changed from equiaxed to plate-like grains, and the size and the aspect ratio of grains increased. This tendency suggests that the growth of grains proceeded predominantly along the directions of the plates, that is, along basal planes of the grains and related to the $\beta \rightarrow \alpha$ phase transformation of SiC during heat treatment. This microstructural development is similar to the formation of plate-like grains in the sintering of β-SiC with addition of Al_2O_3 [9]. The characteristics of the sintered samples are summarized in Table I. Fig. 3 shows a typical microstructure of the boron- and carbon-doped SiC prepared as a reference material for mechanical properties. Similar to the microstructure described in previous reports [17, 18], a microstructural feature with plate-like grains was observed.

3.2. Mechanical properties

The fracture strength of the sintered samples is illustrated in Fig. 4 as a function of holding time. The

TABLE I Characteristics of sintered SiC

	Powder composition	Sintering conditions	Relative density (%)	Grain morphology	Grain size (μm)[a]
B1	90SiC/6Al_2O_3/4Y_2O_3	2000 °C, 1 h	99.1	Equiaxed	1–2.5
B2	90SiC/6Al_2O_3/4Y_2O_3	2000 °C, 2 h	99.2	Equiaxed and plate	2–3 l = 4–8, t = 2–3
B3	90SiC/6Al_2O_3/4Y_2O_3	2000 °C, 3 h	99.0	Plate	l = 6–12, t = 2–4
B5	90SiC/6Al_2O_3/4Y_2O_3	2000 °C, 5 h	98.7	Plate	l = 8–16, t = 3–4
SS	96SiC/3C/1B_4C	2100 °C, 1 h	98.5	Plate	l = 4–13, t = 1–2

[a] l = length of plate-like grain; t = thickness of plate-like grain.

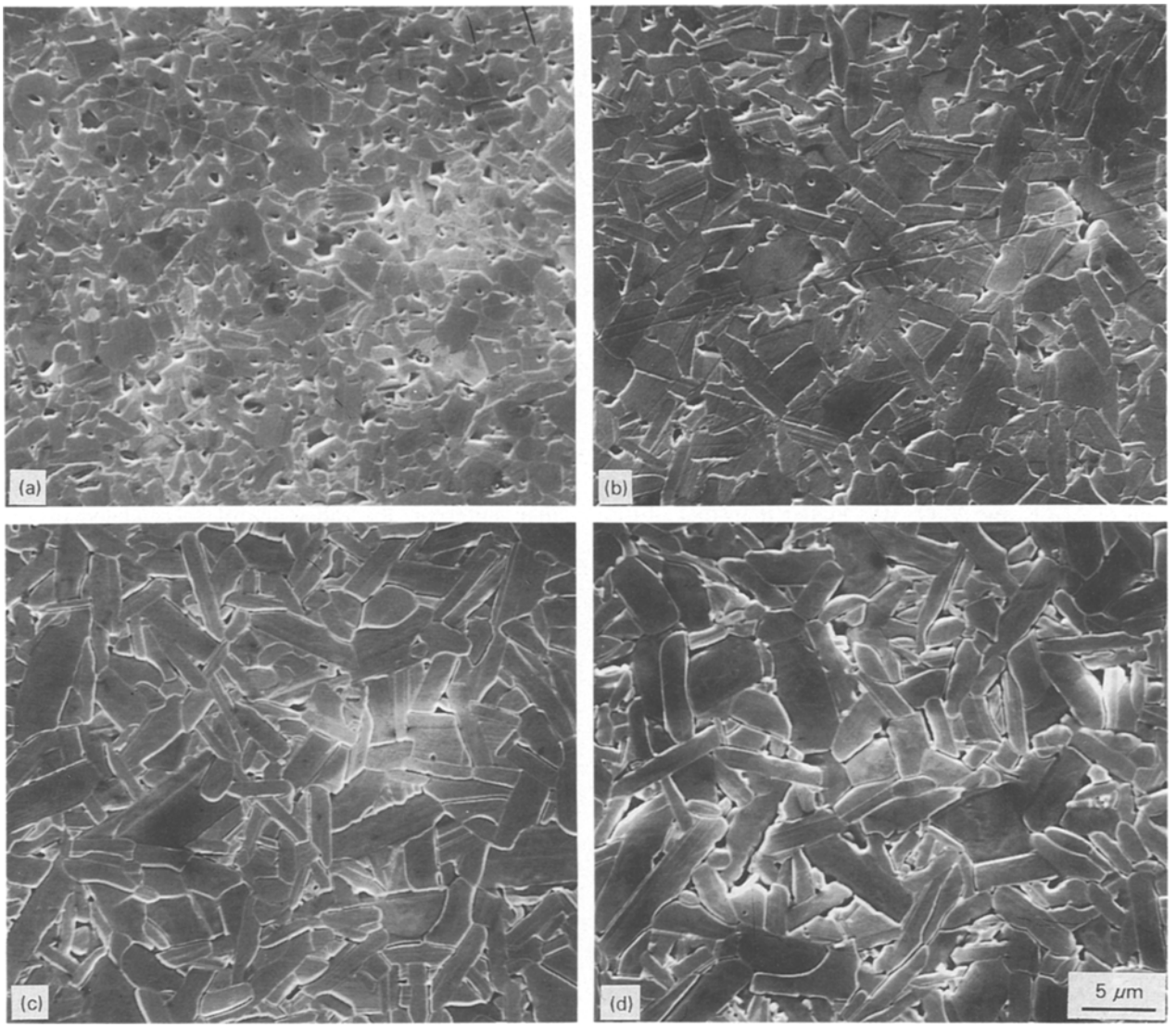

Figure 2 Scanning electron micrographs of the polished and etched surfaces of SiC sintered at 2000 °C with addition of 6 wt% Al_2O_3 and 4 wt% Y_2O_3 for (a) 60, (b) 120, (c) 180, and (d) 300 min.

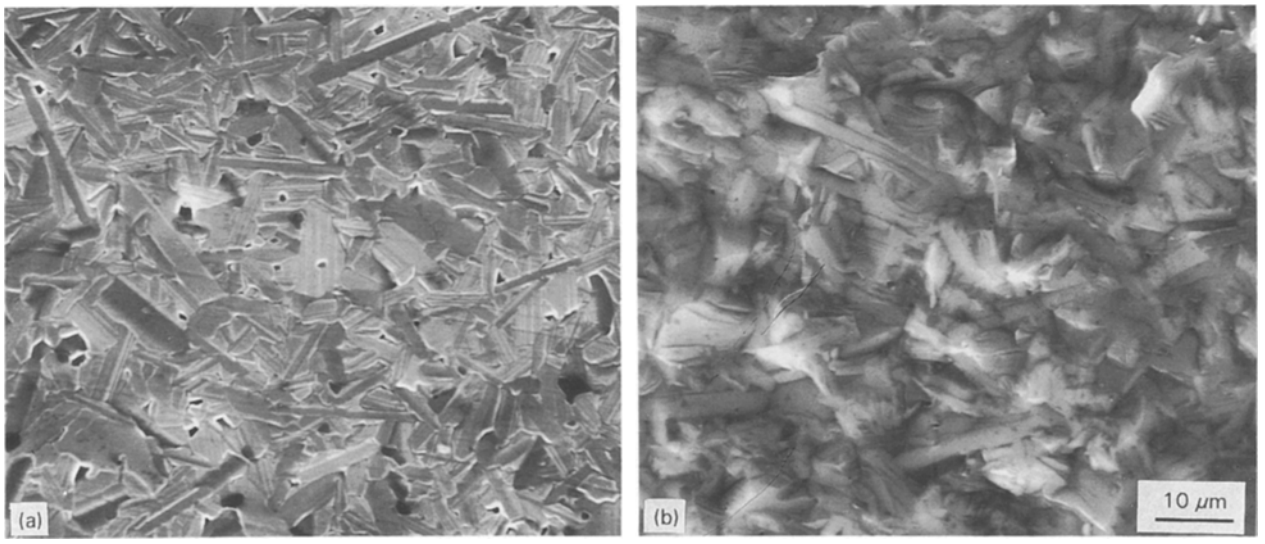

Figure 3 Scanning electron micrographs of (a) the polished and etched surface and (b) the fracture surface of the boron- and carbon-doped SiC.

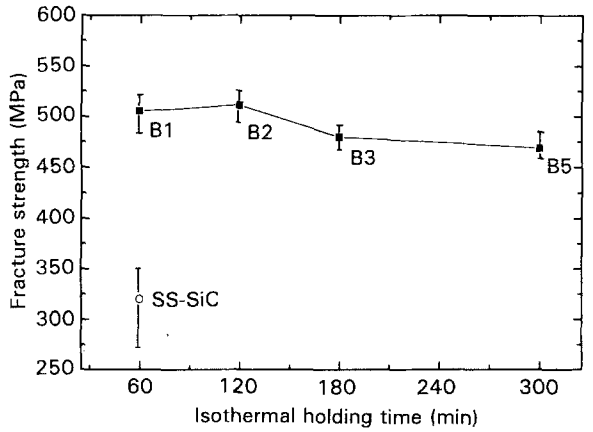

Figure 4 Fracture strength of SiC versus holding time.

fracture strength of the sintered SiC with the addition of Al_2O_3 and Y_2O_3 was higher than that of the boron- and carbon-doped SiC. It has been reported that the fracture strength of the liquid-phase sintered SiC was higher due to uniform microstructural features without large abnormal grains that could act as flaw origins [9, 10]. The fracture strength for the sintered SiC with the addition of Al_2O_3 and Y_2O_3 decreased slightly with holding time. This decrease in strength is considered to be due to grain coarsening. Fig. 5 shows scanning electron micrographs of the fracture surfaces of the sintered SiC with addition of Al_2O_3 and Y_2O_3. The fracture mode in the sintered SiC with the addition of Al_2O_3 and Y_2O_3 was a mixture of intergranular and transgranular. In contrast, the fracture mode in the boron- and carbon-doped SiC was transgranular and predominantly featureless, as shown in Fig. 3b. This phenomenon is related to the characteristics of the grain boundary. The grain boundary for the boron- and carbon-doped SiC is relatively clean without any continuous grain-boundary phase [19, 20]. In the case of the sintered SiC with the addition of Al_2O_3 and Y_2O_3, however, the liquid phases remained along the grain boundaries and at multiple grain junctions [11, 13]. On cooling after sintering, the difference of thermal expansion coefficient between the grain-boundary liquid phase and the matrix (SiC) led to a weak interface and a residual strain field that induced crack deflection [13].

Fig. 6 shows the fracture toughness of the sintered samples versus holding time. The fracture toughness of the boron- and carbon-doped SiC was

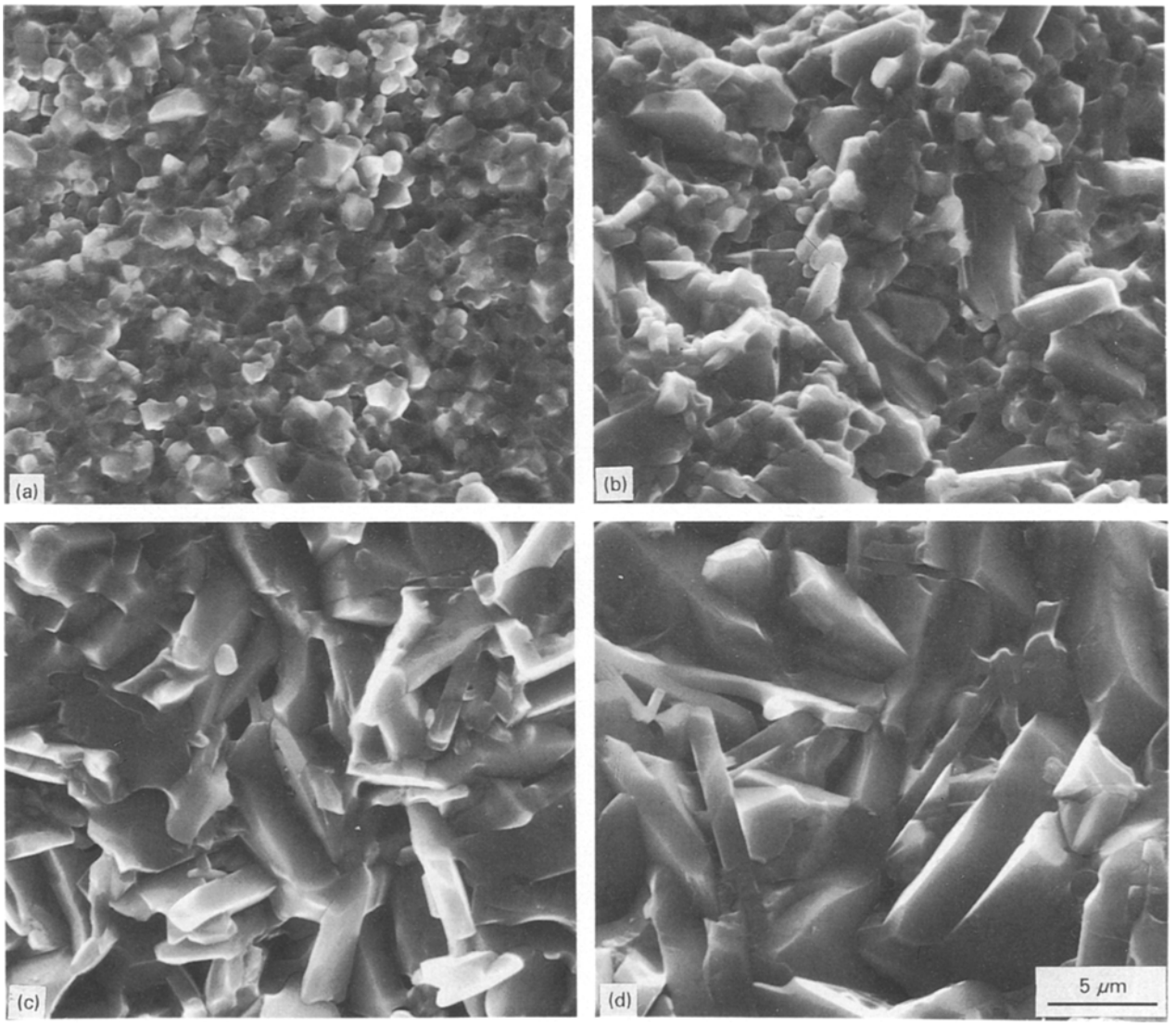

Figure 5 Scanning electron micrographs of the fracture surfaces of SiC sintered at 2000 °C with addition of 6 wt % Al_2O_3 and 4 wt % Y_2O_3 for (a) 60, (b) 120, (c) 180, and (d) 300 min.

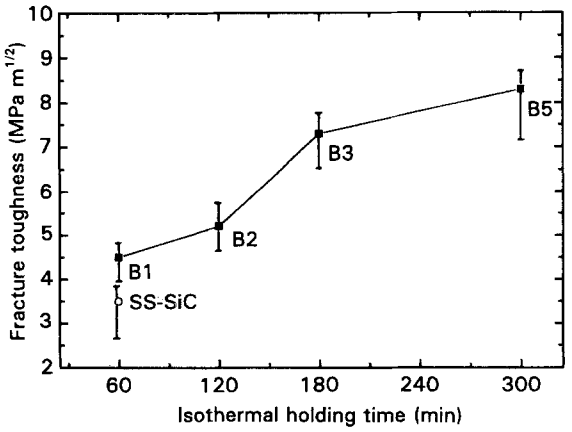

Figure 6 Fracture toughness of SiC versus holding time.

3.5 MPa $m^{1/2}$. The fracture toughness of the sintered SiC with addition of Al_2O_3 and Y_2O_3 was higher than that of the boron- and carbon-doped SiC. This higher value is related to the crack-deflection process. The crack profiles produced at the corners of a Vickers indentation are illustrated in Fig. 7. The crack paths in the boron- and carbon-doped SiC remained planar throughout propagation, as shown in Fig. 7a. However, the sintered SiC with the addition of Al_2O_3 and Y_2O_3 demonstrated significant crack deflection which resulted from a weak interface and/or residual stress (Fig. 7b, c). Therefore, improved fracture toughness of the sintered SiC with the addition of Al_2O_3 and Y_2O_3 compared with the boron- and carbon-doped SiC is considered to be due to the operation of crack deflection. The fracture toughness for the sintered SiC with the addition of Al_2O_3 and Y_2O_3 increased from 4.5 MPa $m^{1/2}$ to 8.3 MPa $m^{1/2}$ with holding time, that is, increasing grain size and aspect ratio. Increased fracture toughness with increasing grain size and aspect ratio can be explained as a crack deflection and bridging operation. A similar trend has been reported for self-reinforcing Si_3N_4 with large elongated grains [21]. Fracture mechanics models predict that the toughening associated with crack deflection should be particle-size invariant but highly dependent on the morphology of the deflecting grains. In particular, elongated grains should be more effective at toughening than equiaxed grains [20, 22]. In addition, crack deflection can lead to the crack bridging which causes a crack closing force behind the crack tip. The effect of crack bridging can be highly enhanced by the formation of elongated grains with a high aspect ratio (e.g. self-reinforcing Si_3N_4) [4, 5, 21, 23, 24]. Fig. 8 shows a micrograph of crack bridging by plate-like grains in SiC with plate-like grains. Therefore, improved fracture toughness is attributed to the crack deflection and crack bridging by the plate-like grains. Fig. 9 shows the grain morphology of the boron- and carbon-doped SiC and the crack-propagation profile. The

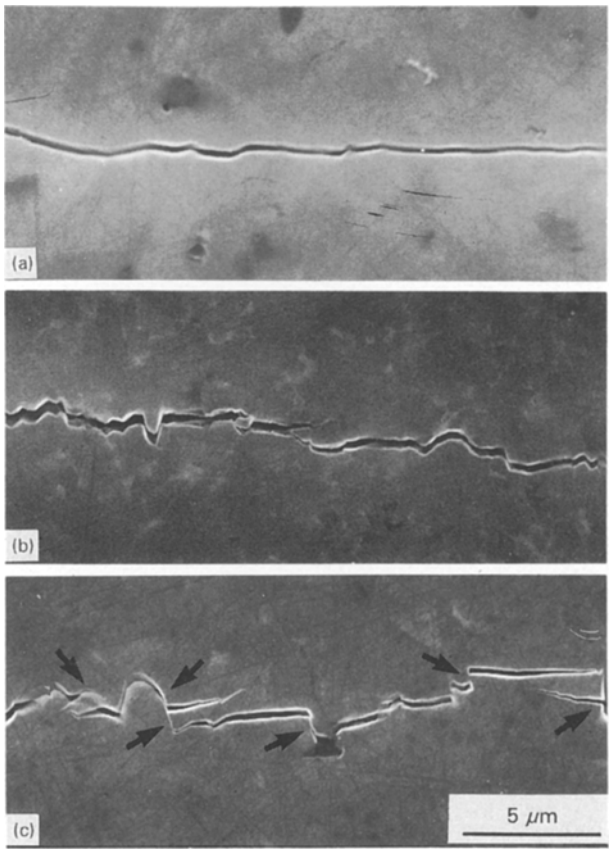

Figure 7 Crack profiles from Vickers indentation cracks in (a) boron- and carbon-doped SiC, SiC sintered at 2000 °C with addition of 6 wt % Al_2O_3 and 4 wt % Y_2O_3 for (b) 60, and (c) 180 min. Note the crack bridging (marked with arrows).

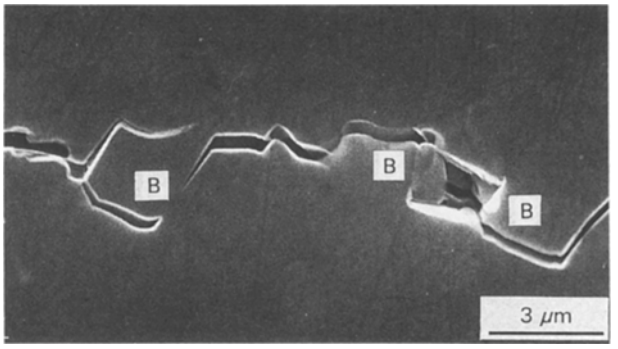

Figure 8 Scanning electron micrograph showing crack bridging in SiC with plate-like grains. B marks crack bridging sites.

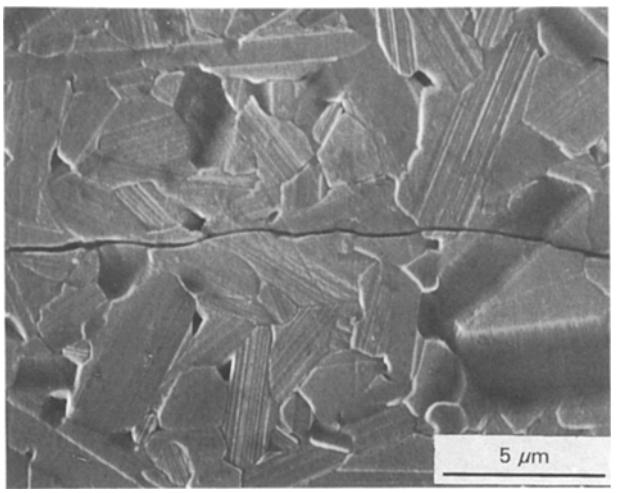

Figure 9 Crack profile induced by Vickers indentation in the boron- and carbon-doped SiC. The surface was etched after indentation.

crack cuts the plate-like grain and propagates almost transgranularly. As a result, fracture toughness is very low, despite a microstructure with plate-like grains. For the boron- and carbon-doped SiC showing a high degree of transgranular fracture, the high aspect ratio of grains may not be very useful in increasing the fracture toughness. Therefore, intergranular fracture is preferentially required to operate crack bridging. These results lead to the conclusion that both the intergranular fracture mode and the elongated grain structure are required to maximize the fracture toughness of the monolithic SiC.

4. Conclusion

SiC ceramic with plate-like grain structure was obtained by pressureless sintering of β-SiC with the addition of 6 wt % Al_2O_3 and 4 wt % Y_2O_3. With increasing holding time, the microstructure changed from equiaxed to plate-like grains through the grain growth associated with the $\beta \rightarrow \alpha$ phase transformation, the size and aspect ratio of the grains increased. With increasing grain size and aspect ratio, fracture toughness increased from 4.5 MPa $m^{1/2}$ to 8.3 MPa $m^{1/2}$ by crack deflection and bridging by plate-like grains.

References

1. S. PROCHAZKA, in "Proceedings of the Conference on Ceramics for High Performance Applications", Hyannes, MA, 1973, edited by J. J. Burke, A. E. Gorum and R. M. Katz (Brook Hill, Chestnut Hill, MA, 1975) pp. 7–13.
2. F. F. LANGE, *J. Am. Ceram. Soc.* **72** (1989) 3.
3. A. G. EVANS, *ibid.* **73** (1990) 187.
4. P. F. BECHER, *ibid.* **74** (1991) 255.
5. M. P. HARMER, H. M. CHAN and G. A. MILLER, *ibid.* **75** (1992) 1715.
6. G. C. WEI and P. F. BECHER, *ibid.* **67** (1984) 571.
7. M. A. JANNEY, *Am. Ceram. Soc. Bull.* **66** (1987) 322.
8. E. TANI, S. UMEBAYASHI, K. KISHI, K. KOBAYASHI and M. NISHIJIMA, *ibid.* **65** (1986) 1311.
9. K. SUZUKI and M. SASAKI, in "Fundamental Structural Ceramics", edited by S. Somiya and R. C. Bradit (Terra Scientific, Tokyo, 1987) pp. 75–87.
10. M. A. MULLA and V. D. KRASTIC, *Am. Ceram. Soc. Bull.* **70** (1991) 439.
11. D. H. KIM and C. H. KIM, *J. Am. Ceram. Soc.* **73** (1990) 1431.
12. M. OMORI and H. TAKEI, *J. Mater. Sci.* **23** (1988) 3744.
13. L. S. SIGL and H.-J. KLEEBE, *J. Am. Ceram. Soc.* **76** (1993) 773.
14. E. M. LEVIN, C. R. ROBBINS and H. F. McMURDIE, in "Phase Diagrams for Ceramists", edited by M. K. Reser (American Ceramic Society, Columbus, OH, 1969) Fig. 2344.
15. J. RUSKA, L. J. GAUCKLER, J. LORENZ and H. U. REXER, *J. Mater. Sci.* **14** (1979) 2013.
16. G. R. ANSTIS, P. CHANTIKUL, B. R. LAWN and D. B. MARSHALL, *J. Am. Ceram. Soc.* **64** (1981) 533.
17. A. H. HEUER, G. A. FRYBURG, L. U. OGBUJI and T. E. MITCHELL, *ibid.* **61** (1978) 406.
18. T. E. MITCHELL, L. U. OGBUJI and A. H. HEUER, *ibid.* **61** (1978) 412.
19. S. PROCHAZKA and C. A. JOHNSON, Final Report, Contract N62269-74-C-0255, G. E. Report No. SRD-74-123 (1974).
20. K. T. FABER and A. G. EVANS, *J. Am. Ceram. Soc.* **66** (1983) C-94.
21. K. MATSTUHIRO and T. TAKAHASHI, *Ceram. Eng. Sci. Proc.* **10** (1989) 807.
22. K. T. FABER and A. G. EVANS, *Acta Metall.* **31** (1983) 565.
23. J. RODEL, *J. Eur. Ceram. Soc.* **8**(9) (1992) 323.
24. *Idem, ibid.* (10) (1992) 143.

Received 31 January
and accepted 21 April 1994